Quantitative Kinetic Investigation on Transmetalation of ArZnX in a Pd-Catalysed Oxidative Coupling

Jing Li,[a] Liqun Jin,[a] Chao Liu,[a] and Aiwen Lei*[a,b]

[a] *College of Chemistry and Molecular Sciences, Wuhan University, Wuhan, 430072, P. R. China*
[b] *State Key Laboratory of Organometallic Chemistry, Shanghai Institute of Organic Chemistry, Chinese Academy of Sciences, 354 Fenglin Lu, Shanghai, 200032, P. R. China*

aiwenlei@whu.edu.cn

Supporting Information

Table of Contents

Analytical methods and reagents.

All reactions and manipulations were conducted in a nitrogen-filled self-prepared three-necked micro reactor. IR spectra were recorded on a Mettler Toledo ReactIR™ 15 spectrometer using a diamond comb. Yields of Ar-Ar were obtained from GC and naphthalene was added as internal standard. All glasswares were oven dried at 120 ^{o}C for more than 1 hour prior to use. THF was dried and distilled from sodium/benzophenone ketyl in nitrogen atmosphere. Anhydrous $ZnCl_2$ was from commercial source (Alfa Aesar 98+%) and used without further purification. $Pd(OAc)_2$ was commercial available. All arylzinc reagents were prepared from the corresponding aryl lithium with $ZnCl_2$ and the concentration was based on the titration by I_2 / LiCl.[1]

Preparation of arylzinc reagents.

To a 100 mL Schlenk flask was added aryl bromide (20 mmol) and THF (7.5 mL) in nitrogen atmosphere. The mixture was allowed to stir at -78 ^{o}C for 5 min. Butyllithium (2.4 M solution in hexanes J&K, 21 mmol) was added slowly via a syringe. 2 h later, the solution of $ZnCl_2$ (24 mmol, in 30 mL THF) was injected to the flask. The mixture temperature was allowed to increase to room temperature. After stirring for about 1 h, the arylzinc reagent concentration was identified based on the titration by I_2 / LiCl.[1]

General procedure of Pd-catalyzed Negishi-type oxidative coupling reactions.

In an oven dried self-prepared three-necked micro reactor with a magnetic stirrer, naphthalene (30 mg) as the internal standard and 2-chloro-1,2-diphenylethanone (0.30 mmol, 69 mg) were added. The reactor was allowed to be vacuumed and purged with nitrogen for several times. The arylzinc reagent (0.35 M in THF （as the solvent）, 4.0 mL) was added in via a syringe. The mixture was allowed to stir at 10 ^{o}C and recorded by React IR. At the same time, $Pd(OAc)_2$ (3.3×10^{-5} M in THF, 60 μL) was added quickly in by a micro syringe. The course of the reaction could be observed from the characteristic IR absorption of 2-chloro-1,2-diphenylethanone or product.When 2-chloro-1,2-diphenylethanone was consumed completely, or the product did not increase, the reaction was quenched by diluted hydrochloric acid and the yield of product was determined by GC.

Other reactions followed the same procedure under different reaction conditions.

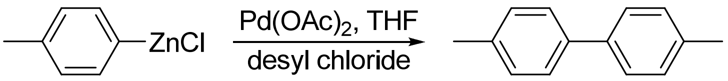

1a **2a**

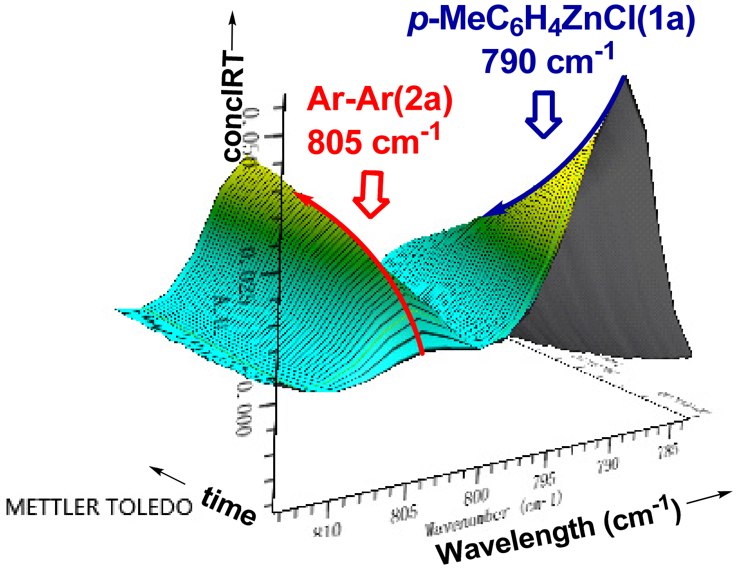

Figure S1 The characteristic IR absorptions of homocoupling of *p*-MeC_6H_4ZnCl and *p*-MeC_6H_4ZnCl.

Following general procedure, the course of the reactions was observed from the characteristic IR absorption of homocoupling of organozinc reagent.

Kinetic studies of Pd-catalyzed Negishi-type oxidative homo-coupling of *p*-MeC_6H_4ZnCl under different concentrations of catalyst.

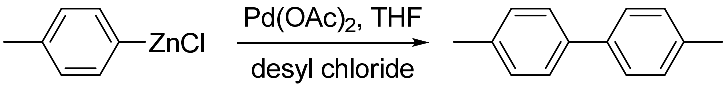

1a **2a**

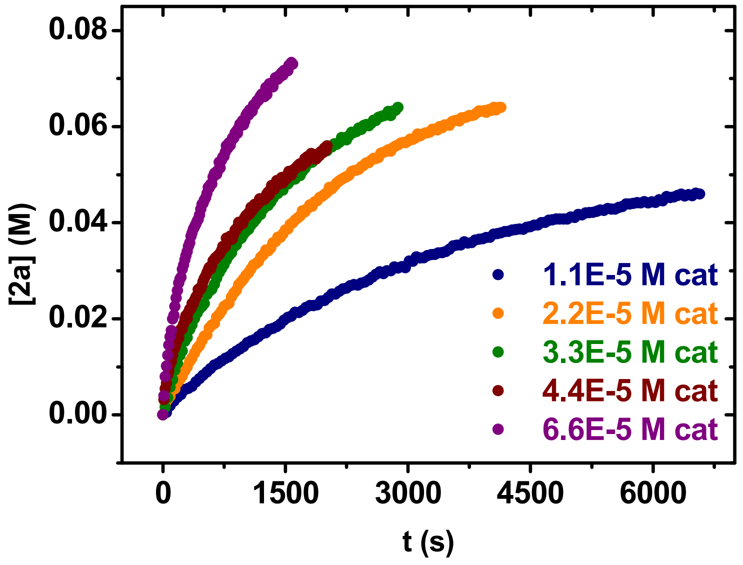

(A)

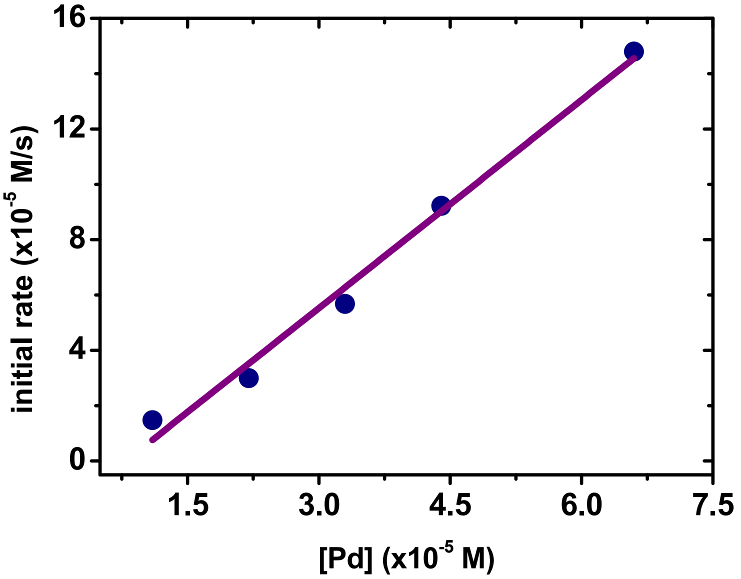

(B)

Figure S2 Kinetic profiles of the oxidative homocoupling of *p*-MeC_6H_4ZnCl (**1a**) (0.35 M in THF, 4.0 mL) under different concentrations of $Pd(OAc)_2$ (1.1×10^{-5}M–6.6×10^{-5} M), 2-chloro-1,2-diphenylethanone (**3a**) (7.5×10^{-2} M in THF, 0.3 mmol), -20 °C.

Following general procedure, kinetic experiments of Pd-catalyzed homocoupling of **1a** under different concentrations of palladium have been carried out. According to Figure S2, it was revealed that with the concentration of palladium changing from

1.1×10^{-5} M to 6.6×10^{-5} M, plotting the initial rates *vs* [Pd] obtained a linear relationship, suggesting that the reaction was first-order dependent on Pd concentration ([Pd]≦ 6.6×10^{-6} M) (Figure S2 (B)).

Kinetic studies of Pd-catalyzed Negishi-type oxidative homocoupling of *p*-MeC_6H_4ZnCl under different concentrations of arylzinc.

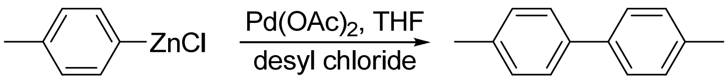

1a **2a**

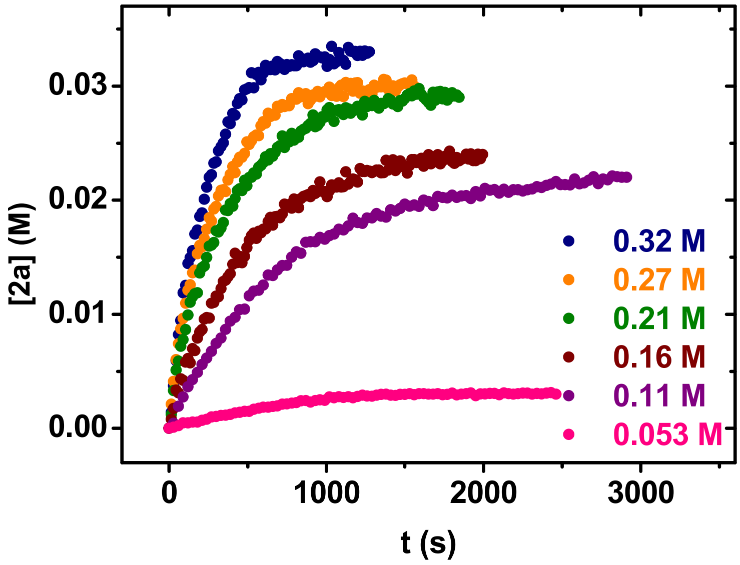

(A)

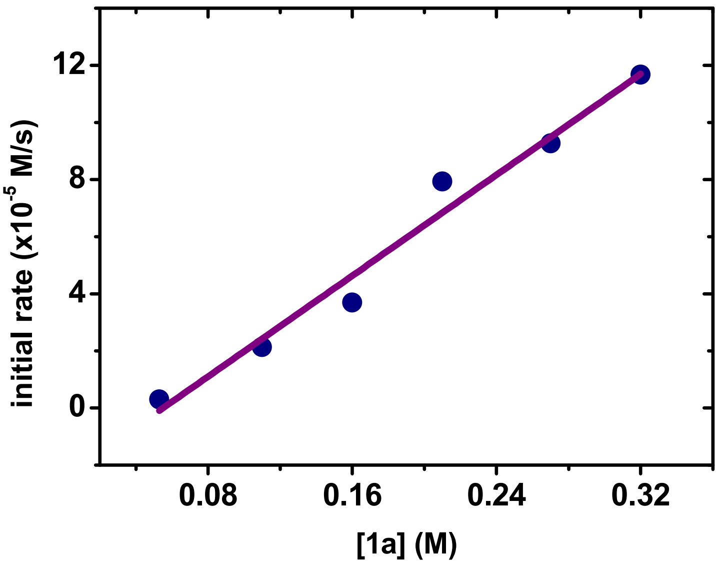

(B)

Figure S3. Kinetic profiles of the oxidative homocoupling of p-MeC$_6$H$_4$ZnCl (**1a**) (0.053 M–0.32 M in THF, 6.0 mL), 2-chloro-1,2-diphenylethanone (**3a**) (5.0×10^{-2} M in THF, 0.3 mmol), Pd(OAc)$_2$ (3.3×10^{-5} M in THF), 30 °C.

Following the general procedure, the oxidative homo-coupling reactions with different concentrations of arylzinc were carried out, and the kinetic profiles were shown in the Figure S3. It was clearly shown that plotting the initial rates *vs* [**1a**] obtained a linear relationship (Figure S3 (B)). In other words, the reaction displayed first-order dependent on [**1a**].

Kinetic studies of Pd-catalyzed Negishi-type oxidative homocoupling of *p*-MeC$_6$H$_4$ZnCl under different concentrations of 2-chloro-1,2-diphenylethanone.

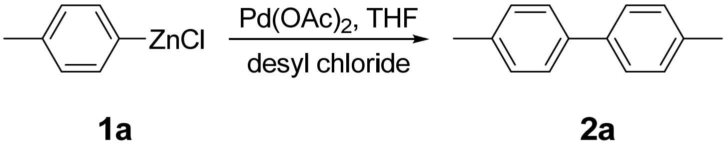

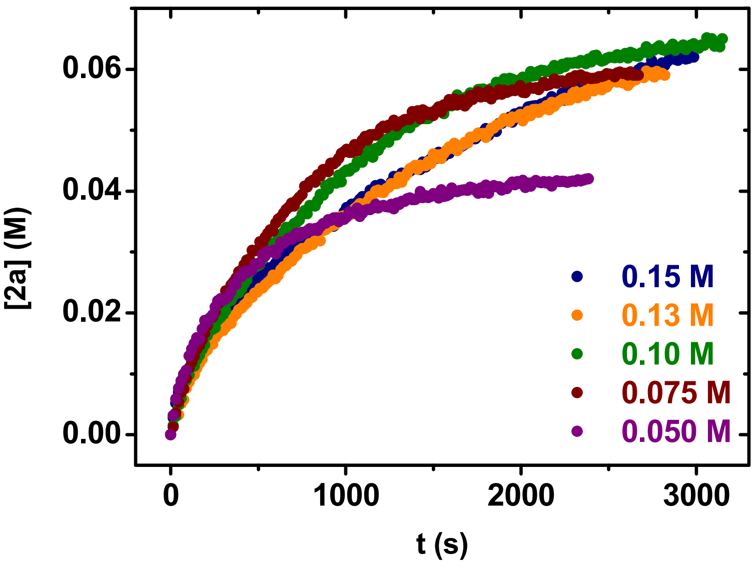

(A)

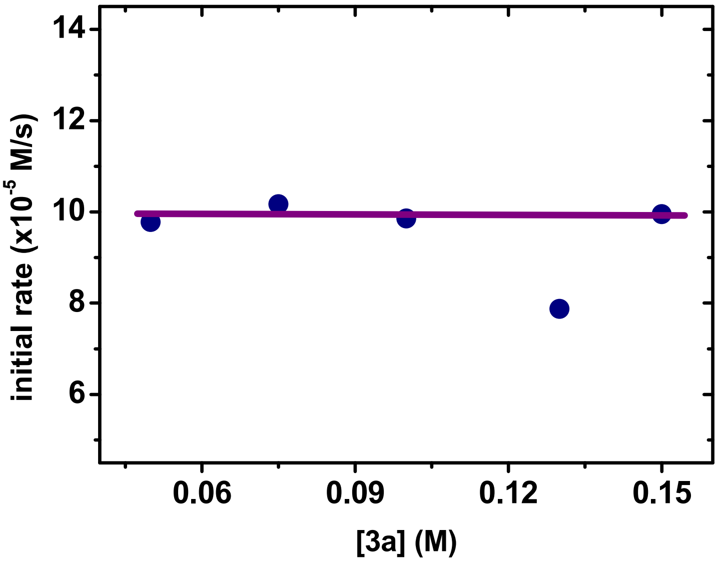

(B)

Figure S4. Kinetic profiles of the oxidative homocoupling of *p*-MeC$_6$H$_4$ZnCl (**1a**) (0.31 M in THF, 4.0 mL), 2-chloro-1,2-diphenylethanone (**3a**) (0.050 M–0.15 M in THF), Pd(OAc)$_2$ (3.3×10^{-5} M in THF), 10 ^{o}C.

Following the general procedure, the oxidative homo-coupling reactions with different concentrations of [**3a**] were carried out; the kinetic profiles were shown in the Figure S4, respectively. It was clearly shown that the initial rates were identical with the variation of the concentrations of [**3a**]. In other words, the reaction displayed zero-order kinetic behavior of [**3a**]. So the transmetalation should be the rate-limiting step according to the Figure S3 and Figure S4.

Kinetic studies of Pd-catalyzed Negishi-type oxidative homocoupling of *p*-MeC_6H_4ZnCl at different temperatures.

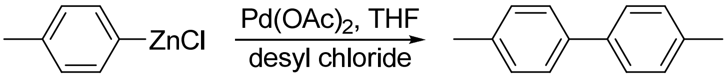

1a **2a**

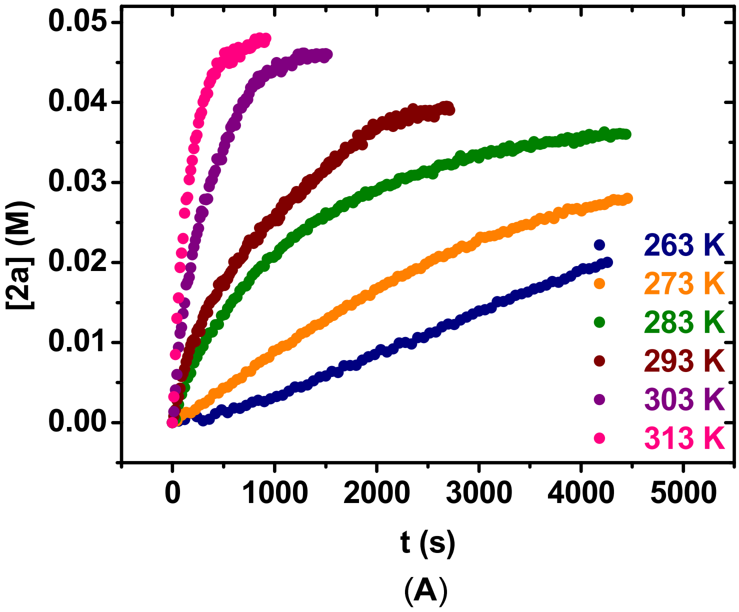

(A)

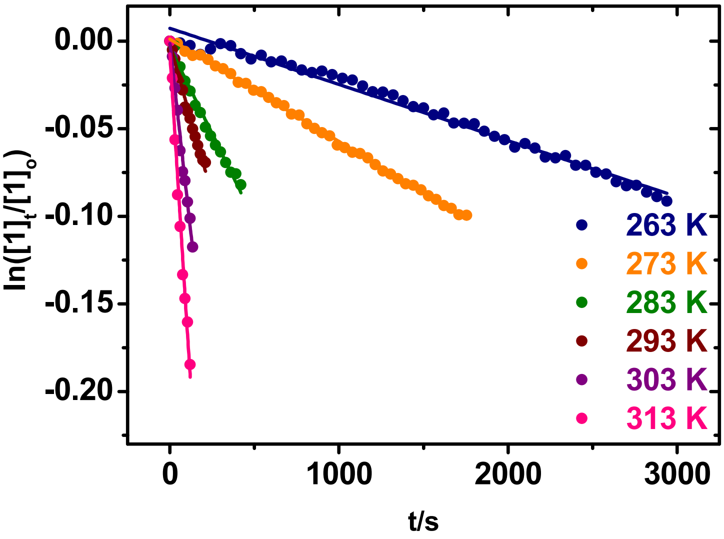

(B)

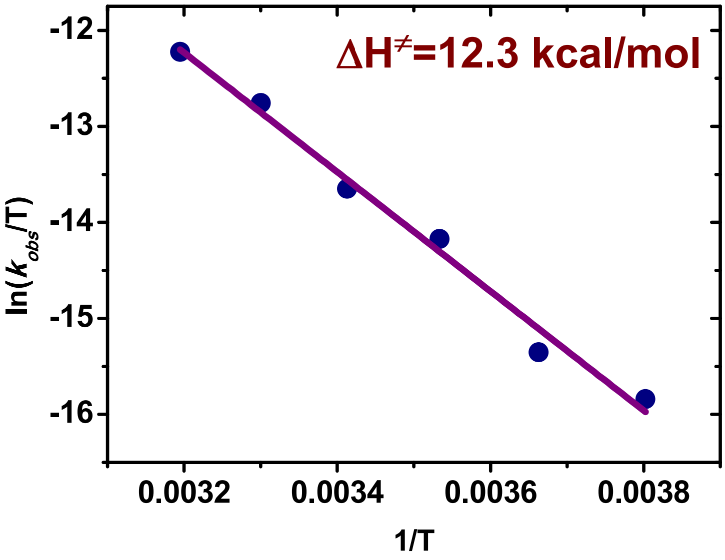

(C)

Figure S5 Kinetic investigation of Pd-catalyzed oxidative homocoupling of *p*-MeC_6H_4ZnCl (**1a**) at different temperatures. 2-chloro-1,2-diphenylethanone (**3a**) (7.5×10^{-2} M in THF, 0.3 mmol), *p*-MeC_6H_4ZnCl (**1a**) (0.31 M in THF, 4.0 mL), $Pd(OAc)_2$ (3.3×10^{-5} M in THF). **(A)** Kinetic plots of [**2a**] *vs* t. **(B)** Kinetic plots of ln ([**1a**]$_t$/[**1a**]$_0$) *vs* t. **(C)** Plots of ln (k_{obs}/T) *vs* (1/T).

Following the general procedure, these reactions were carried out under different temperatures. According to the concentration of product, the concentration of *p*-Me C_6H_4ZnCl could be derived as the formula:

$$[\mathbf{1a}] = [\mathbf{1a}]_{t=0} - 2\times[\mathbf{2a}]$$

The rate constants k_{obs} could be obtained plotting ln ($[\mathbf{1a}]_t/[\mathbf{1a}]_0$) *vs* t (Figure S5 (B)). Plots of ln (k_{obs}/T) *vs* (1/T) gave a linear relationship. According to Eyring equation, the activation enthalpy $\Delta H^{\neq}$ could be obtained (Table S1).

Table S1 Kinetic parameters

According to Eyring Equation:

$$\ln\frac{k}{T} = -\frac{\Delta H^{\neq}}{R}\times\frac{1}{T} + \ln\frac{k_B}{h} + \frac{\Delta S^{\neq}}{R}$$

T (K)	k_{obs} (s^{-1})	1/T (K^{-1})	ln(k_{obs}/T)	$\Delta H^{\neq}$ (kcal/mol)
263	3.47E-5	3.80E-3	-15.84	**12.3**
273	5.86E-5	3.66E-3	-15.35	
283	1.98E-4	3.53E-3	-14.17	
293	3.45E-4	3.41E-3	-13.65	
303	8.74E-4	3.30E-3	-12.76	
313	1.54E-3	3.19E-3	-12.22	

Kinetic studies of Pd-catalyzed Negishi-type oxidative homocoupling of different arylzinc reagents.

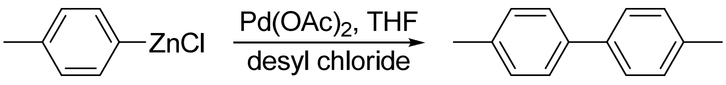

1a

2a

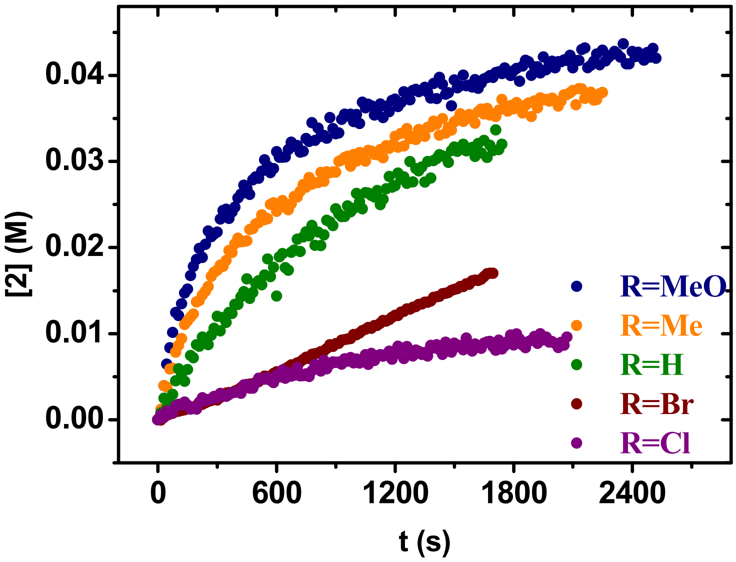

(**A**)

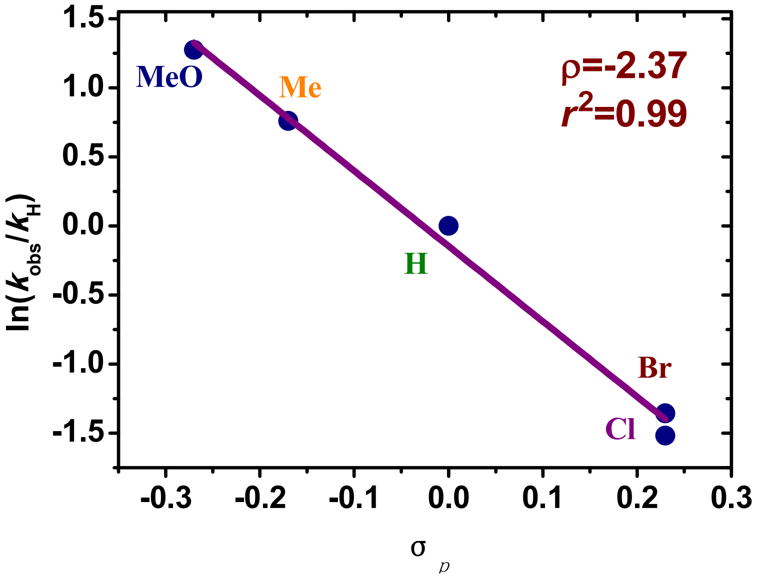

(**B**)

Figure S6 (**A**) Kinetic profiles of [**2**] *vs* t in Pd(OAc)$_2$-catalyzed oxidative homo-coupling of different arylzinc reagents. 2-chloro-1,2-diphenylethanone (**3a**) (7.5×10^{-2} M in THF, 0.3 mmol), ArZnCl (0.30 M in THF, 4.0 mL), Pd(OAc)$_2$ (2.8×10^{-5} M in THF), 10 ^{o}C. (**B**) Hammett correlation.

Pd-catalyzed oxidative homocoupling reactions with *p*-MeOC$_6$H$_4$ZnCl, *p*-Me C$_6$H$_4$ZnCl, C$_6$H$_5$ZnCl, *p*-BrC$_6$H$_4$ZnCl and *p*-ClC$_6$H$_4$ZnCl were carried out according to the general procedure. As shown in Figure S6, a linear free energy relationship was observed with a calculated ρ-value of -2.37. The electron-efficient arylzinc reagent displayed faster reaction rates than electron-deficient arylzinc reagent. The result further supported that the transmetalation was the rate-limiting step.

Kinetic studies of Pd-catalyzed Negishi-type oxidative homocoupling of *p*-MeC_6H_4ZnCl under different oxidants.

As shown in scheme 1: there are two theoretical paths for this reaction to get the homocoupling product of ArZnCl. For the path 1, oxidative addition of RCl to Pd(0) affords [R-Pd-Cl], the subsequent transmetalation between **1a** and **TM-I** furnishes the intermediate [Ar-Pd-R]. Then, the second transmetalation between **1a** and **II-1** forms [Ar-Pd-Ar], and the reductive elimination of [Ar-Pd-Ar] produces Ar-Ar. For the path 2, oxidative addition of RCl to Pd(0) affords [R-Pd-Cl], the subsequent transmetalation between **1a** and **TM-I** furnishes the intermediate [Ar-Pd-Cl]. Then, the second transmetalation between **1a** and **II-2** forms [Ar-Pd-Ar], and the reductive elimination of [Ar-Pd-Ar] produces Ar-Ar. Pd-catalyzed oxidative homocoupling reactions under different oxidants were carried out according to the general procedure.

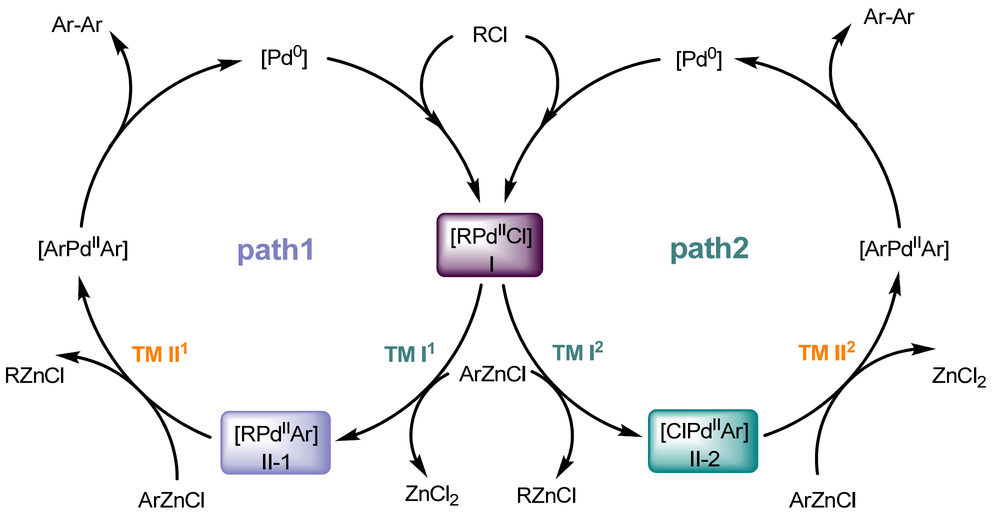

Scheme 1 The Pd-catalyzed oxidative homocoupling reaction

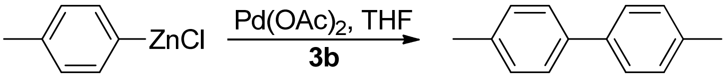

1a **2a**

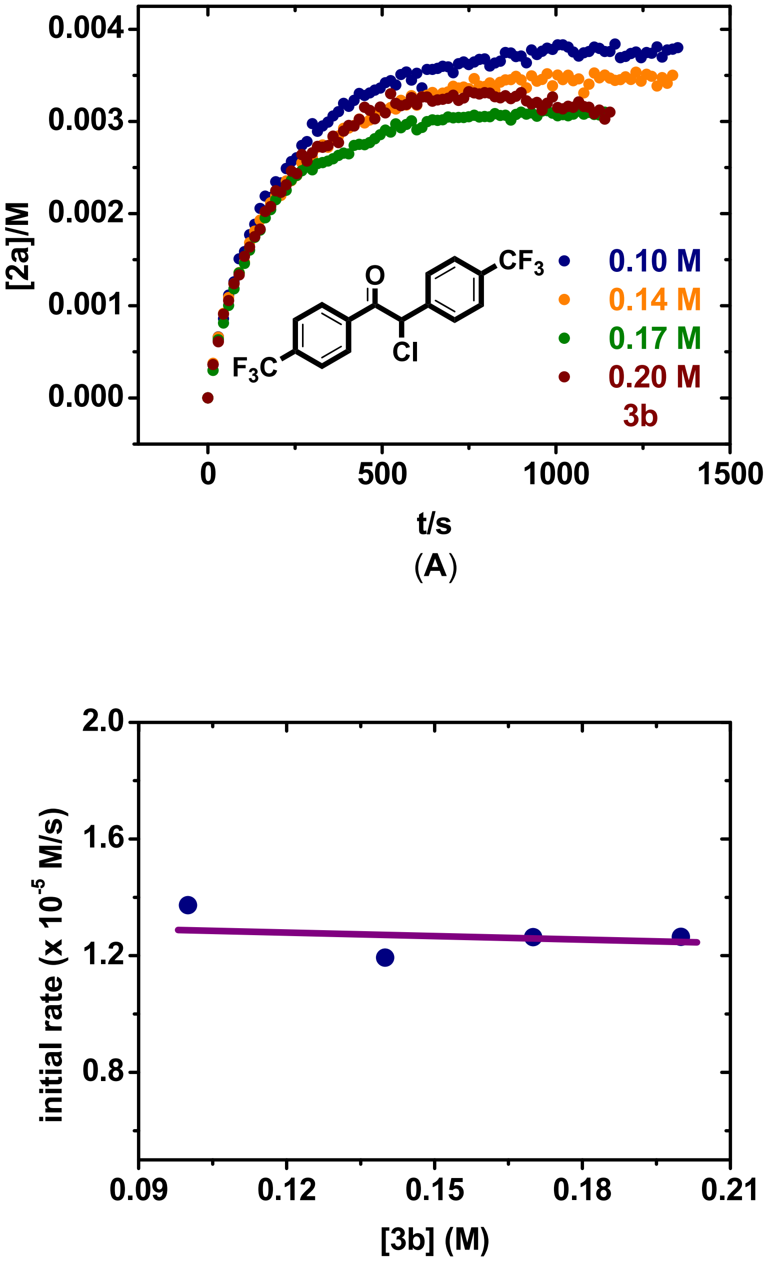

(A)

(B)

Figure S7-1 Kinetic profiles of [**2a**] *vs* t in Pd(OAc)$_2$-catalyzed oxidative homo-coupling of *p*-MeC$_6$H$_4$ZnCl with different concentration of **3b**. **3b** (0.10 M–0.20 M in THF), *p*-MeC$_6$H$_4$ZnCl (0.35 M, 4.0 mL), Pd(OAc)$_2$ (5.6×10^{-5} M in THF), 10 ^{o}C.

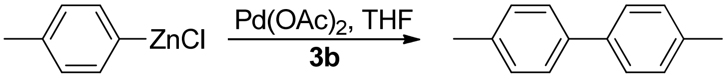

1a **2a**

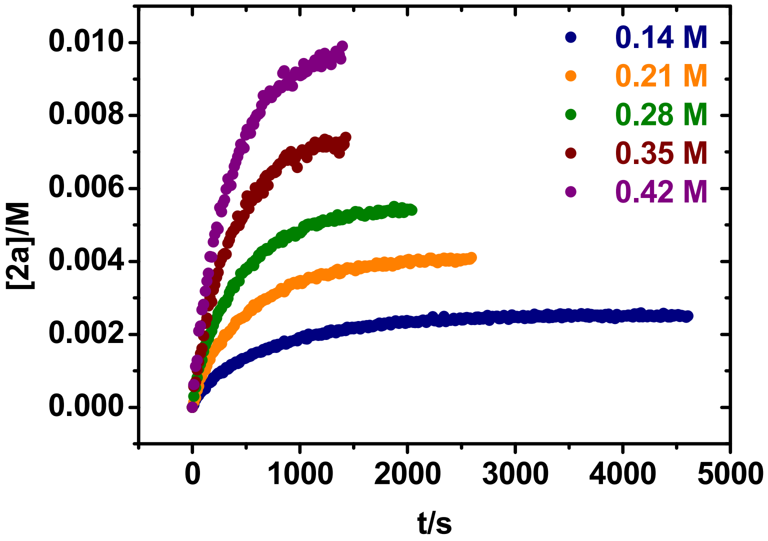

(**A**)

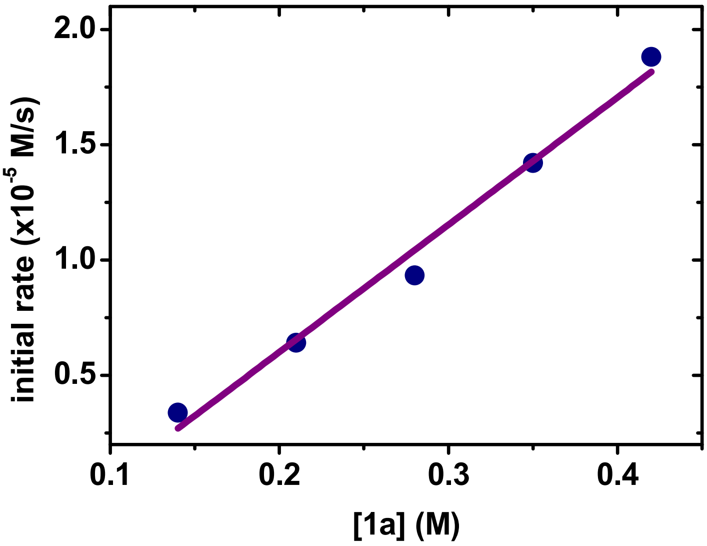

(**B**)

Figure S7-2 Kinetic profiles of [**2a**] *vs* t in Pd(OAc)$_2$-catalyzed oxidative homo-coupling of *p*-MeC$_6$H$_4$ZnCl with **3b** as oxidant. **3b** (6.8×10^{-2} M in THF, 0.41 mmol), *p*-MeC$_6$H$_4$ZnCl (0.14

M–0.42 M, 6.0 mL), Pd(OAc)$_2$ (3.7×10^{-5} M in THF), 0 °C.

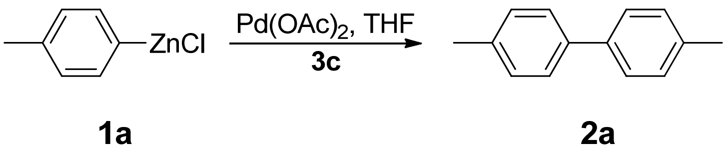

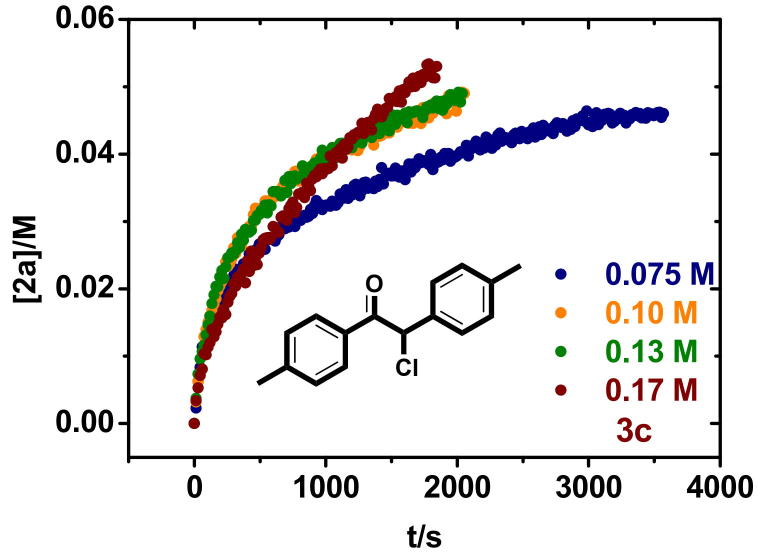

(**A**)

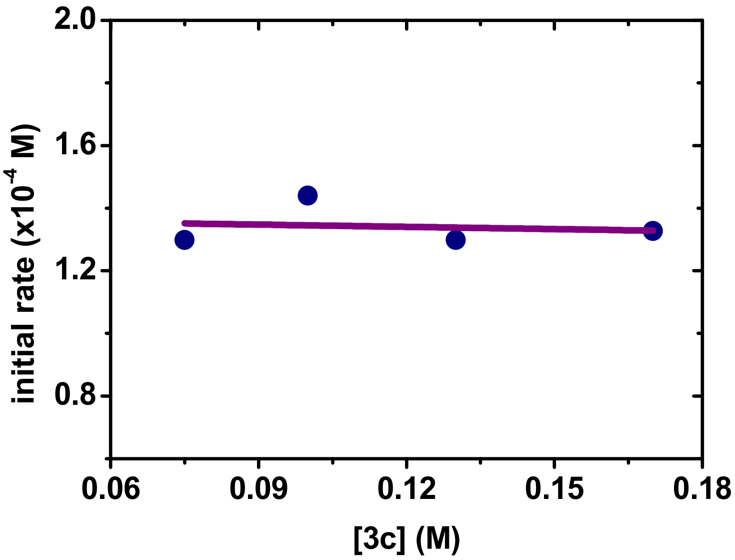

(**B**)

Figure S7-3 Kinetic profiles of [**2a**] *vs* t in Pd(OAc)$_2$-catalyzed oxidative homo-coupling of *p*-MeC_6H_4ZnCl with different concentration of **3c**. **3c** (7.5×10^{-2} M–1.7×10^{-1} M in THF), *p*-MeC_6H_4ZnCl (0.35 M, 4.0 mL), $Pd(OAc)_2$ (5.6×10^{-5} M in THF), 10 °C.

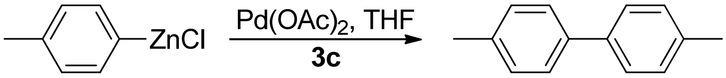

1a **2a**

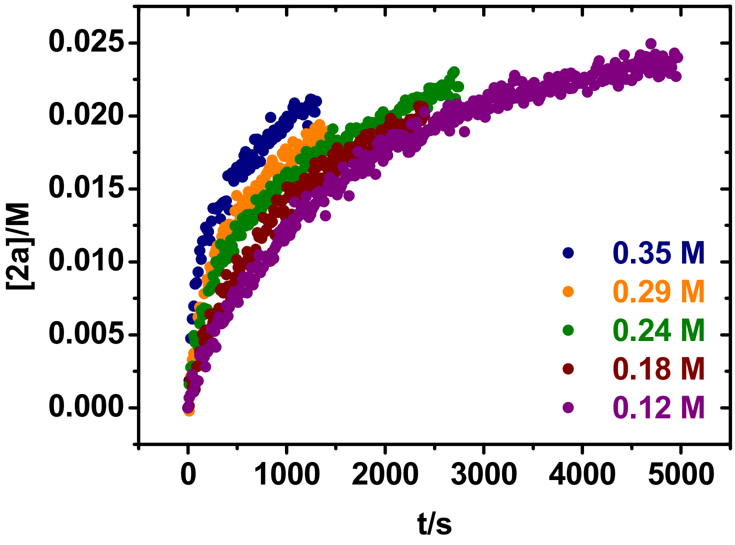

(**A**)

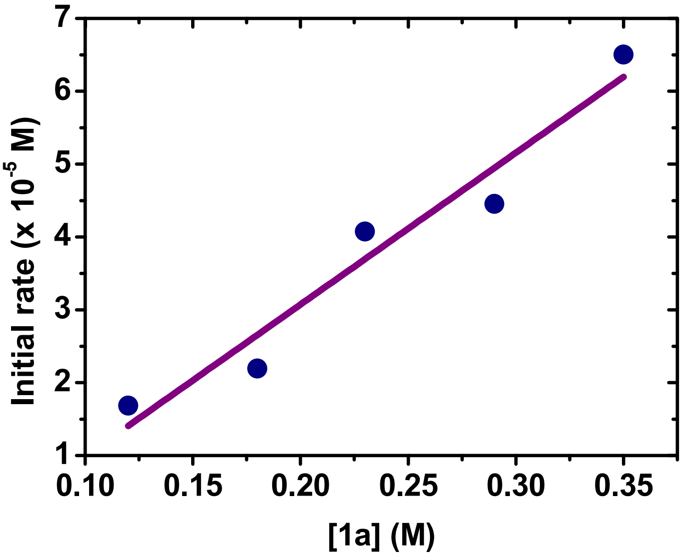

(**B**)

Figure S7-4 Kinetic profiles of [**2a**] *vs* t in Pd(OAc)$_2$-catalyzed oxidative homo-coupling of *p*-MeC$_6$H$_4$ZnCl with **3c** as oxidant. **3c** (5.1×10^{-2} M in THF, 0.31 mmol), *p*-MeC$_6$H$_4$ZnCl (0.12 M–0.35 M, 6.0 mL), Pd(OAc)$_2$ (3.7×10^{-5} M in THF), 10 °C.

Following the general procedure, we detected the kinetic behavior of different oxidants. As shown in Figure S7-1 the reaction displayed zero-order on [**3b**], indicating that oxidative addition was not the rate-limiting step. As shown in Figure S7-2, the reaction displayed first-order on [**1a**]. Hence, the transmetalation was the rate-limiting step. When **3c** was used, same kinetic behavior was determined. In other words, by employing different substituted oxidants, the rate limiting step points to the transmetalation. As shown in Figure S7-5, when employing different oxidants (**3a**, **3b**, **3c**), varied initial rates could be observed, demonstrating that II-1 was involved in the rate-limiting step, which should be assigned to TM II^1 in path 1.

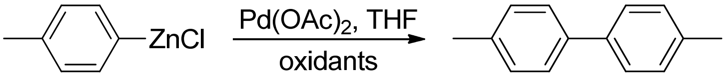

1a **2a**

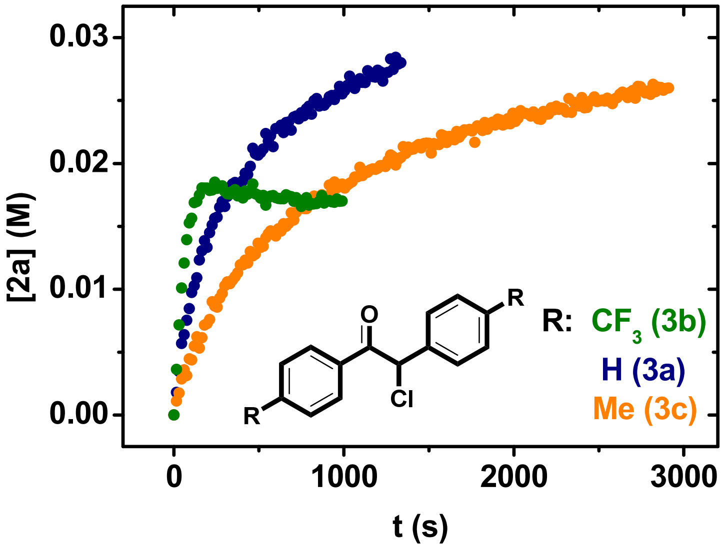

Figure S7-5 Kinetic profiles of [**2a**] *vs* t in Pd(OAc)$_2$-catalyzed oxidative homocoupling of *p*-MeC$_6$H$_4$ZnCl (0.27 M in THF, 4.0 mL). Oxidants (**3a**, **3b**, **3c**) (5.0×10^{-2} M in THF, 0.2 mmol), Pd(OAc)$_2$ (2.8×10^{-5} M in THF), 10 °C.

References

(1) Krasovskiy, A.; Knochel, P. *Synthesis* **2006**, 890-891.